Thermoluminescence of nitrogen–neon and nitrogen–argon nanoclusters immersed in superfluid helium

Adil Meraki

Department of Physics, Bilecik Seyh Edebali University, Bilecik, Turkey

TUBITAK National Metrology Institute, Gebze, Turkey

Patrick T. McColgan, Sergei Sheludiakov, David M. Lee, and Vladimir V. Khmelenko

Department of Physics and Astronomy and Institute for Quantum Science & Engineering, Texas A&M University,
College Station, TX 77843, USA
E-mail: khmel@physics.tamu.edu

Ensembles of nanoclusters created by injection of nitrogen atoms and molecules as well as rare gas (RG) atoms (Ne and Ar) into superfluid ^{4}He have been studied via optical and electron spin resonance (ESR) spectroscopies. We studied the dynamics of thermoluminescence spectra emitted during the warming of porous structures formed by nitrogen–neon and nitrogen–argon nanoclusters inside superfluid helium. We show experimental evidence that quantum vortices initiate chemical reactions in porous ensembles of nanoclusters. Using this experimental approach, it is possible to study chemical reactions of heavy atoms and molecules at very low temperatures where normally their diffusion and quantum tunneling in solid matrices are completely suppressed.

Keywords: thermoluminescence, porous structures, nanoclusters, superfluid helium.

1. Introduction

Investigations of thermoluminescence of solid nitrogen containing stabilized nitrogen atoms have a long history. According to the mechanism first proposed by Edwards [1], warming up of the sample initiates diffusion of stabilized nitrogen atoms through a solid matrix leading to recombination when atoms occupy neighboring sites in the N_2 matrix. Products of this recombination are excited nitrogen molecules which relax to the metastable $A^3\Sigma_u^+$ state and emit light ($A^3\Sigma_u^+ - X^1\Sigma_g^+$, Vegard–Kaplan (VK) bands), or their excitation energy can be transferred to stabilized nitrogen atoms through chains of N_2 molecules. Excited nitrogen atoms emit α-group (transition $^2D - ^4S$) and δ-group (transition $^2P - ^2D$) radiation. In earlier work it was found that emission starts at $T \sim 5$ K and continues upon warming to 36 K [2–4]. Three maxima of thermoluminescence at $T \sim 16$, 20 and 23 K were observed. These maxima were explained by three types of traps with different activation energies needed for leaving these traps [4,5]. Concentrations of stabilized nitrogen atoms in solid N_2 did not exceed 0.03% in these experiments [3]. Thermoluminescence of nitrogen atoms was also studied in nitrogen–neon [6–8] and nitrogen–argon solids [6,9].

Completely different temperature dependences of thermoluminescence were observed in collections of molecular nitrogen nanoclusters formed in bulk superfluid helium. Local concentrations of nitrogen atoms stabilized in molecular nitrogen nanoclusters were substantially larger, up to 30% [10]. The ensembles of nanoclusters were formed by injection of products of a discharge in nitrogen–helium gas mixtures into bulk superfluid helium [11,12]. The nanoclusters form a porous gel-like material inside superfluid helium [13,14]. Each nanocluster is coated with a few layers of solid helium which impedes the recombination of stabilized atoms. X-ray studies gave estimates of average sizes of nanoclusters in the range 3–10 nm and an overall density of impurity atoms and molecules of order 10^{20} cm^{-3} [13–17]. Ultrasound studies showed a wide distribution of pore sizes from 8 to 860 nm [14]. Most of the stabilized nitrogen atoms reside on the surfaces of nanoclusters [18,19].

In contrast to the earlier experiments with N_2 samples, thermoluminescence of ensembles of molecular nitrogen nanoclusters containing high concentrations of stabilized atoms usually started after raising temperature from 1.5 K [20]. In the first experiments, upon warming, the effect of thermal explosions of nanoclusters with intense peaks of luminescence was observed during passage through the λ-point

($T \sim$ 2.17 K) of liquid helium [11,20]. Two maxima of thermoluminescence were observed, one at T = 2.17 K and another at T = 3.8 K. These values of temperature are smaller than those observed in solid nitrogen.

Thermoluminescence was studied when ensembles of nanoclusters were immersed in liquid helium and when samples were removed from liquid helium. For the latter case two maxima of thermoluminescence were observed. The temperature of both maxima of thermoluminescence were dependent on the pressure of helium vapor in the Dewar [21]. For pressures of helium vapor equal to 10 torr the maxima were observed at 2.5 and 4.5 K. When pressure in the Dewar was allowed to grow from 10 to 100 Torr, the maxima were observed at 8 and 10 K [21].

As a consequence of high concentrations of nitrogen atoms, extracting nanoclusters from superfluid helium led to explosive recombination of nitrogen atoms and destruction of nanoclusters. During the destruction of nanoclusters the temperature was increasing from 1.5 to 15 K. Dynamics of thermoluminescence during destruction of molecular nitrogen nanoclusters were studied in our earlier experiments [22,23]. It was found that at the onset of destruction the fusion of nanoclusters was accompanied with emission of the α-group of nitrogen atoms and the VK bands of N_2 molecules. At the final stage of destruction the emission of the β-group of O atoms, the M- and β-bands of NO molecules and the second Herzberg bands of O_2 molecules became dominant [23]. Oxygen was present in these experiments as a result of a small impurity ($\sim 10^{-6}$) in the helium gas used for formation of nanoclusters in He II.

Even more surprising results were obtained during investigations of thermoluminescence of ensembles of nanoclusters immersed in superfluid helium. First, it was observed that afterglow of nanoclusters in the samples lasted much longer than that in solid molecular nitrogen [24]. Second, small step heating of nanoclusters immersed in He II led to the appearance of luminescence of nitrogen atoms and molecules. Thermoluminescence was explained by capturing single metastable $N(^2D)$ atoms and N_2 molecules in solidified helium during the process of accumulation of the sample and their diffusion in solid helium resulting in the formation of the complexes $N(^2D)$–N_2 [24]. Recently another mechanism was suggested for explanation of thermoluminescence of nanoclusters immersed in He II [25]. It was suggested that electrons and nitrogen ions can be captured in nanoclusters during their accumulation in He II. Small increases of temperature might initiate release of electrons from the shallow traps. The electrons can tunnel through solid nitrogen and be attracted to nitrogen ions. As a result of electron-ion recombination, the excited N_2 molecules can be formed which provide energy for observed thermoluminescence.

From another point of view, the behavior of nanoclusters immersed in He II might be influenced by the properties of superfluid helium. One of the remarkable features of superfluid helium is formation of quantized vortices during application of a heat flux. Recently investigations of quantum vortices and quantum turbulence attracted great attention [26–28]. Considerable progress in this area has been obtained due to new experimental methods. For example, the visualization of quantum vortices was realized [29–33]. By using visualization of vortex cores, the observation of the reconnection of vortices and direct observation of Kelvin waves excited by quantum vortex reconnection had been made [34,35]. The influence of vortices on the process of coalescence of nanoparticles in liquid helium was also studied [36,37].

In our previous work we studied the temperature dependence of the thermoluminescence of ensembles of nitrogen nanoclusters immersed in He II and found that maximum of thermoluminescence coincided with the maximum of density of quantum vortices for the conditions of our experiments [38]. The thermoluminescence was explained by recombination of nitrogen atoms residing on surfaces of nanoclusters. The recombination occurs in the quantum vortices, which attract the nanoclusters. When nanoclusters are entrained into vortex cores, the rate of collision of nanoclusters is increased substantially. That explains why the temperature dependence of thermoluminescence follows the temperature dependence of vortex density in He II.

In present work we performed experiments with ensembles of nitrogen–neon and nitrogen–argon nanoclusters containing stabilized nitrogen atoms. We observed a temperature dependence of thermoluminescence of these nanoclusters in He II with maxima at $T \sim$ 1.9 K similar to that observed for ensembles of nitrogen nanoclusters [38]. In the thermoluminescence spectra of nitrogen–neon and nitrogen–argon nanoclusters immersed in He II the α-group of N atoms, β-group of O atoms, VK and first positive system bands of N_2 molecules and M-bands of NO molecules were registered. These results provide additional evidences that thermoluminescence of nanoclusters immersed in He II is initiated by quantum vortices. We discuss possible mechanisms for thermoluminescence initiated by quantum vortices.

2. Experimental method

The experimental setup for simultaneous optical and electron spin resonance (ESR) studies of nanoclusters with stabilized free radicals at low temperatures has been described in more detail elsewhere [39]. The ESR measurements were performed with a Bruker spectrometer operating in the *X*-band (8.91 GHz) equipped with a Janis liquid helium cryostat, whose tail was centered between the pole faces of a homogeneous Varian 7800 electromagnet. The Janis cryostat contained a variable temperature insert (VTI), which was thermally insulated from the main 4 K helium bath. The ESR measurements were conducted for samples immersed in superfluid helium at $T \sim$ 1.32 K which can be

achieved by pumping on the VTI with a roots blower backed by a mechanical pump.

Figure 1 shows an experimental setup for formation and optical and ESR studies of atoms contained in the collections of nanoclusters. Gas mixtures containing N_2 and neon or argon along with helium were prepared in a container at room temperature and transported through a Mass Flow Controller (a Brooks Model 5850E) with a constant flux of $5 \cdot 10^{19}$ particles/s to the cryogenic region. When the prepared gas mixtures passed through a quartz capillary surrounded by liquid nitrogen, high-power radio-frequency ($f \sim 53$ MHz, power ~ 75 W) was applied to electrodes which were placed around the lower portion of the capillary to dissociate the nitrogen molecules.

The presence of the helium gas in the gas mixture increased the efficiency of dissociation of the N_2 molecules in the discharge due to the interaction of the energetic metastable helium atoms and molecules with N_2 molecules. A gas jet was created as the mixed gases passed through an orifice with diameter 0.75 mm at the bottom of the quartz capillary. The jet impinged on the surface of superfluid helium contained in a small beaker 20–25 mm below

Fig. 1. (Color online) Schematic of the setup for optical spectroscopy and electron spin resonance studies of the ensembles of nanoclusters immersed in superfluid helium: *1* — cryostat, *2* — magnet, *3* — lens for collecting light emitted from the sample, *4* — optical stage, *5* — fiber optics, *6* — quartz tube, *7* — discharge electrodes, *8* — teflon blade, *9* — liquid helium level meter, *10* — microwave cavity with optical access, *11* — modulation coil, *12* — sample collection beaker, *13* — ruby crystal.

the orifice. A fountain pump placed at the bottom of the liquid helium bath in the VTI maintained a constant level of superfluid helium in the beaker. Once the jet meets cold helium vapor evaporating from the liquid helium, formation of nanoclusters containing nitrogen molecules and N and O atoms trapped in the clusters took place. Argon or neon atoms had also been introduced into the sample gases and were thus contained in the nanoclusters. The presence of oxygen in the samples, as we mentioned earlier, is due to the small contamination of oxygen (1 ppm) in the helium gas. The jet penetrated through the superfluid He surface and a gel-like sample was created. This process continued as the sample was accumulated on the conical part of the beaker. A set of teflon blades was employed to scrape the sample from the walls of the funnel while the beaker was rotated so that all of the sample collected onto the funnel surface fell into the cylindrical part of the beaker. Sample accumulation lasted 10 min. During the sample formation, the temperature was maintained at $T = 1.5$ K by using a needle valve connecting VTI with the main helium bath.

Once we had accumulated ~0.3–0.4 cm^3 of sample in the cylindrical part of the beaker, sample accumulation was terminated, and the beaker was lowered into the ESR cavity by a pair of sliding tubes. Further details of the homemade cylindrical copper cavity can be found elsewhere [39]. All ESR signals were detected for samples immersed in superfluid helium at ~1.32 K. The modulation frequency was set at 100 kHz, and derivatives of the ESR absorption lines were obtained at a magnetic field ~0.32 T by a lock-in amplifier.

Double integration of the ESR spectra gave the number of atoms stabilized by comparison with the signal from a ruby crystal (under the same experimental conditions) mounted at the bottom of the microwave cavity and oriented so that the ruby ESR signal did not overlap with the sample ESR signal. The calibration of the signal from the ruby crystal was made by reference to a diphenyl-picrylhydrazil (DPPH) sample, with a known number of spins $\sim 2.4 \cdot 10^{-17}$. ESR measurements were initially performed, providing an estimate of the average and local concentrations of $N(^4S)$ atoms.

The average concentrations were determined from the number of stabilized atoms in the samples measured by ESR and the volume 0.35 cm^3 occupied by the samples in the ESR cavity. The local concentrations were estimated from ESR line widths which were increased due to dipole-dipole interactions of electron spins of nitrogen atoms [19]. After that we ceased pumping on the helium vapor from the sample reservoir, and let the temperature rise from $T \sim 1.32$ to 2.16 K. The temperature of the sample was recorded with a germanium thermometer attached to the top of the cavity. Warming up the nitrogen–neon/argon–helium condensates led to the appearance of rather intense thermoluminescence. The emitted light passes along the fused silica quartz cylinder in the cavity, then through the holes in
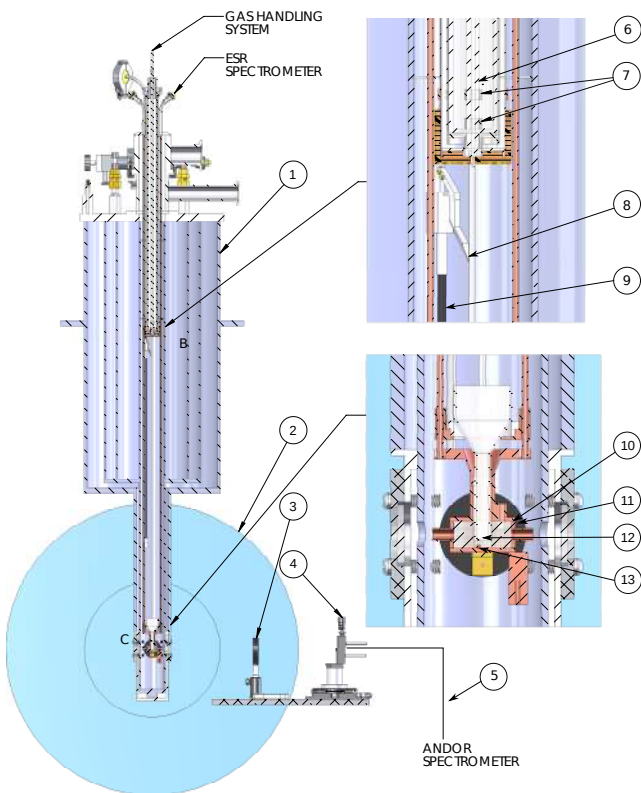
the cavity, and finally through the quartz window in the cryostat.

The window material and the fused silica quartz are transparent for the wavelength range 200–1100 nm. The emitted light was guided to the optical fiber with the help of the lens. The fiber then transferred light to the entrance of the Andor spectrometer. The Andor spectrometer consists of the Shamrock SR-500i spectrograph, with a 0.52 nm (1st grating) resolution, equipped with a cooled EM-CCD (Newton 970) camera. The emission spectra are detected by the Andor spectrometer with a 150 lines/nm grating (blaze wavelength 500 nm), and a wavelength range of 340 nm (mostly in the wavelength range 240–580 nm) with a Newton CCD detector unit cooled to –60 °C. For registration of the thermoluminescence spectra during the sample warm up, the exposure time was 50 ms. We opened the main pumping line just before passing the λ-point and cooled down the liquid helium with the sample to the initial temperature $T \sim 1.32$ K and again performed ESR detection of stabilized nitrogen atoms.

3. Experimental results

3.1. Studies of thermoluminescence during warming up of ensembles of nitrogen–argon nanoclusters immersed in superfluid helium

We studied thermoluminescence of ensembles of nitrogen–argon nanoclusters containing stabilized nitrogen atoms during the warm up from 1.32 to 2.16 K. After performing the registrations of ESR for as-prepared samples at $T = 1.32$ K, the samples were heated to 2.16 K by ceasing pumping on the helium vapor from the VTI. It is worth noting that the samples remain inside the superfluid helium during the entire period of warming up. Dynamics of the thermoluminescence of nitrogen–argon nanoclusters prepared from the gas mixture [N$_2$]/[Ar]/[He] = 1/1/200 is presented in Fig. 2(a). Figure 2(b) shows the integrated intensity of the spectra detected during the thermoluminescence process. The integrated spectrum consists of intense VK molecular bands N$_2(A^3\Sigma_u^+, 0 \to X^1\Sigma_g^+, v'')$, the luminescence of the α-group of atomic nitrogen N($^2D \to ^4S$), and the β-group emission of atomic oxygen O($^1S \to ^1D$). In addition to above-mentioned bands, weak β″-groups of O atoms can be seen as a result of simultaneous vibration excitation of N$_2$ molecules and emission of O atoms. Figure 2(c) presents the time dependences of α-group, VK bands, and β-group intensities as well as time dependence of sample temperature during warming from 1.32 to 2.16 K. It can be seen from Fig. 2(c), that there are maxima of the intensity of thermoluminescence which occur at $T \sim 1.9$ K for all three lines.

The observation of maxima in the intensity of thermoluminescence at $T \sim 1.9$ K may hold the key to understanding the nature of thermoluminescence at very low temperatures. Therefore, we performed studies of the behavior of the thermoluminescence dynamics for ensembles of nano-
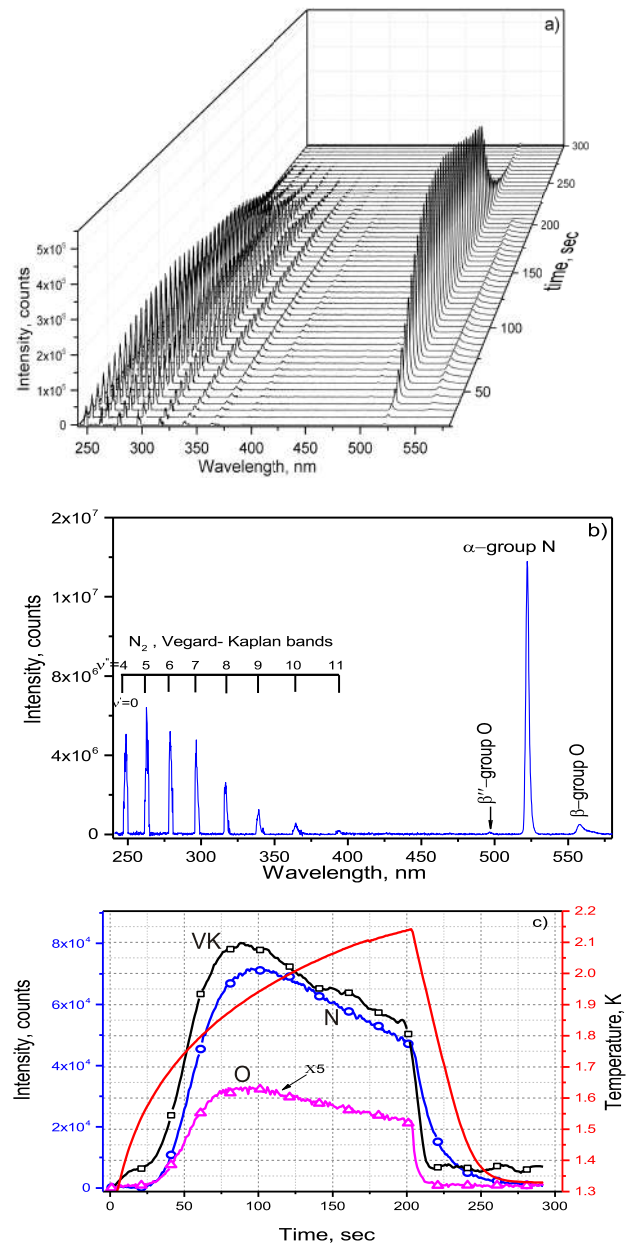

Fig. 2. (Color online) Thermoluminescence of ensemble of nitrogen–argon nanoclusters immersed in superfluid helium. An ensemble of nanoclusters was prepared from gas mixture [^{14}N$_2$]/[Ar]/[He] = 1/1/200. (a) Dynamics of thermoluminescence spectra of the ensemble of nanoclusters during warming up from 1.3 to 2.15 K. Each spectrum in the figure is a sum of 100 spectra taken with exposure time 50 ms. (b) Integrated thermoluminescence spectra obtained during entire warming process. (c) Time dependence of sample temperature (red line). Time dependences of thermoluminescence intensity for nitrogen molecules integrated over all observed VK bands (black line with squares), nitrogen atoms (blue line with circles) and oxygen atoms (magenta line with triangles).

clusters prepared from gaseous mixtures of different compositions. Figure 3 shows the temperature dependences of thermoluminescence for ensembles of nanoclusters formed by injecting of [N$_2$]/[Ar]/[He] gas mixtures with different
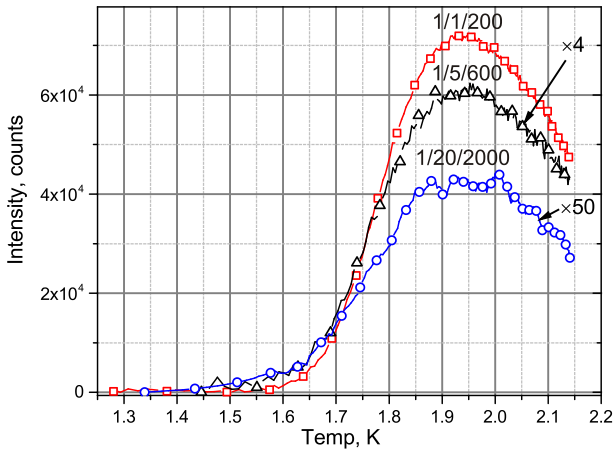
Fig. 3. (Color online) Temperature dependences of thermoluminescence intensity of nitrogen atoms for ensembles of nanoclusters formed from different nitrogen–argon–helium gas mixtures: 1/1/200 (red line with squares), 1/5/600 (black line with triangles) and 1/20/2000 (blue line with circles). Warm up to $T \sim 2.15$ K lasted 202, 165, and 215 s, respectively.

ratios. In Fig. 3 the intensity of thermoluminescence for ensembles of nanoclusters prepared from gas mixtures $[N_2]/[Ar]/[He] = 1/5/600$ and $[N_2]/[Ar]/[He] = 1/20/2000$ were increased for comparison purposes by a factor of 4 and 50, respectively, as indicated on Fig. 3. The position of the peak as a function of temperature does not change for the all three samples studied. Figure 4 also shows the integrated spectra of thermoluminescence of three different ensembles of nitrogen–argon nanoclusters which were formed from $^{14}N_2/Ar/He$ gas mixtures during warming.
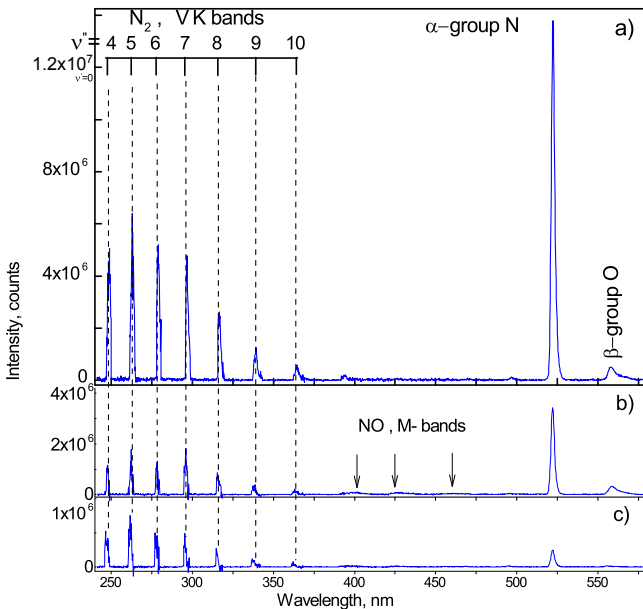

Fig. 4. Integrated thermoluminescence spectra obtained during warming of three ensembles of nitrogen–argon nanoclusters. Ensembles of nitrogen–argon nanoclusters were prepared from different $[^{14}N_2]/[Ar]/[He]$ gas mixtures: (a) 1/1/200, (b) 1/5/600, (c) 1/20/2000.

3.2. Studies of thermoluminescence during warming up of ensembles of nitrogen–neon nanoclusters immersed in superfluid helium

We also investigated the effect of adding different quantities of Ne atoms to the nitrogen–helium gas mixture on the behavior of the luminescence of N atoms in IHCs. Figure 5(a) presents the dynamics of the thermoluminescence
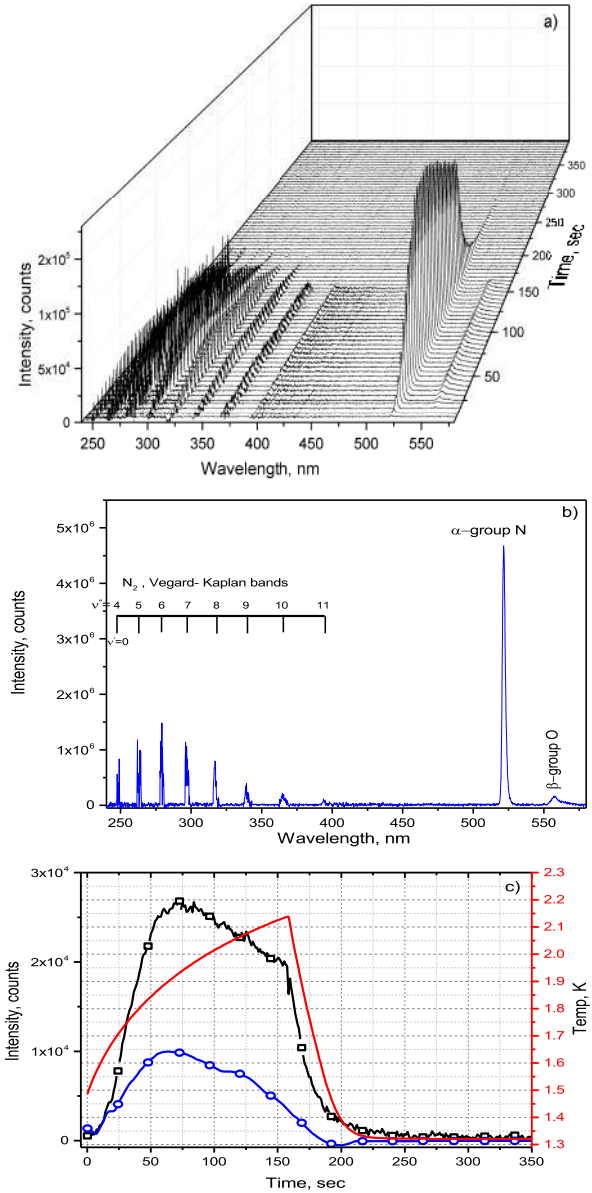

Fig. 5. (Color online) Thermoluminescence of nitrogen–neon nanoclusters immersed in superfluid helium. Nanoclusters were prepared from gas mixture $[^{14}N_2]/[Ne]/[He] = 1/1/100$. (a) Dynamics of thermoluminescence spectra of the nanoclusters during warming up from 1.3 to 2.15 K. Each spectrum in the figure is a sum of 100 spectra taken with exposure time 50 ms. (b) Integrated thermoluminescence spectra obtained during entire warming process. (c) Time dependences of sample temperature (red line). Time dependence of thermoluminescence intensity for VK bands of nitrogen molecules (blue line with circles), and α-group of nitrogen atoms (black line with squares).

of a nitrogen–neon–helium sample prepared from the gas mixture $[^{14}N_2]/[Ne]/[He] = 1/1/100$. The integrated intensity of the spectra obtained during the thermoluminescence process is shown in Fig. 5(b). Figure 5(c) shows the time dependence of intensity of the α-group of N atoms and the VK bands of N_2 molecules. The intensities of the α-group and VK bands for this sample are smaller due to the lower average concentration of N atoms ($5 \cdot 10^{18}$ cm^{-3}) in contrast to the sample formed from 1/1/200 in the case of nitrogen–argon–helium gas mixtures, where the average concentration of N atoms is equal to $1 \cdot 10^{19}$ cm^{-3}. The N atom concentrations were determined by ESR.

The integrated spectra of thermoluminescence of three different samples which were formed from $^{14}N_2$/Ne/He gas mixtures during warm up are shown in Fig. 6. Although only the α-, β-groups and VK bands are detected for the sample prepared from the gas mixture $[^{14}N_2]/[Ne]/[He] = 1/1/100$, in the case of the samples prepared from $[^{14}N_2]/[Ne]/[He] = 1/20/400$ and $[^{14}N_2]/[Ne]/[He] = 1/50/1000$ gas mixtures, M bands of NO molecules are also present in the integrated spectra of thermoluminescence. For the case of sample prepared from the gas mixture $[^{14}N_2]/[Ne]/[He] = 1/1/100$ and $[^{14}N_2]/[Ne]/[He] = 1/50/1000$, the optical spectra were obtained in the spectral range 240–580 nm. The spectral range is 300–640 nm for the sample formed from the $[^{14}N_2]/[Ne]/[He] = 1/20/400$ gas mixture. As can be seen from Fig. 6(b), the bands at ~589 nm and ~629 nm are present in the spectrum. These bands were assigned to the $B^3\Pi_g - A^3\Sigma_u^+$ transition of N_2 molecules.

The temperature dependences of thermoluminescence for samples formed by injecting different nitrogen–neon–
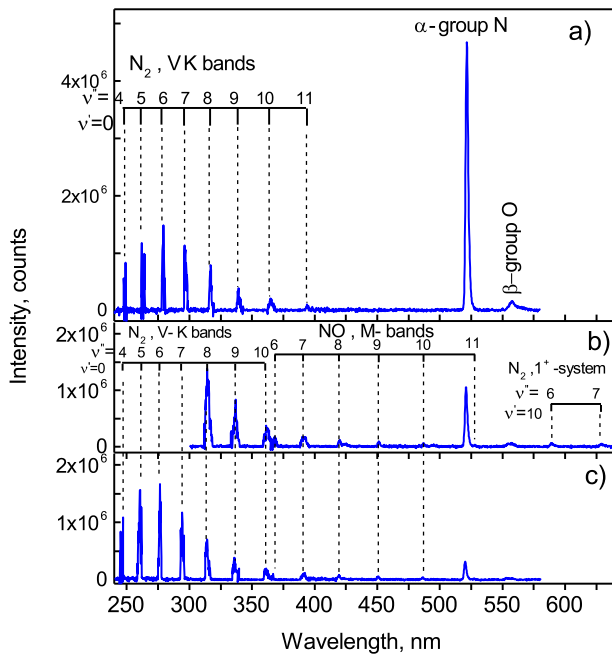
Fig. 6. (Color online) Integrated luminescence spectra obtained during warming of three ensembles of nitrogen–neon–nanoclusters. Nitrogen-neon nanoclusters were prepared from $[^{14}N_2]/[Ne]/[He]$ gas mixtures: (a) 1/1/100, (b) 1/20/400, (c) 1/50/1000.
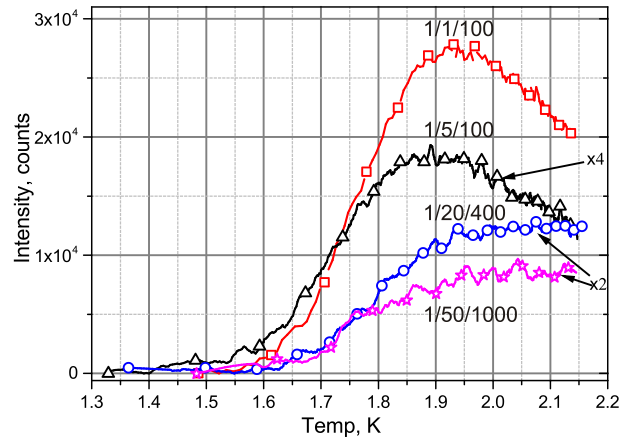
Fig. 7. (Color online) Temperature dependences of thermoluminescence intensity of nitrogen atoms in nitrogen–neon nanoclusters formed from different nitrogen–neon–helium gas mixtures: 1/1/100 (red line with squares), 1/5/100 (black line with triangles) and 1/20/400 (blue line with circles), 1/50/1000 (magenta line with stars). Warming up to $T \sim 2.15$ K lasted 157, 212, 255, and 227 s, for curves from top to bottom, respectively.

helium gas mixtures are shown in Fig. 7. The observed intensities of thermoluminescence from the samples prepared from gas mixtures $[^{14}N_2]/[Ne]/[He] = 1/5/100$, 1/20/400, and 1/50/1000 were increased by a factor of 4, and 2, respectively, as displayed in Fig. 7. The maxima of the intensity of thermoluminescence are at $T \sim 1.9$ K for the two upper curves in Fig. 7. For the two lower curves the maxima are shifted to higher temperature. In the samples which correspond to the two lower curves in Fig. 7, the nitrogen atoms were stabilized mostly in a neon matrix. The lifetimes of different components of the α-group emission of nitrogen atoms stabilized in a neon matrix are substantially larger (up to ~350 s) than that of nitrogen atoms in nitrogen and argon matrices (~ 30 s) [24]. When the lifetimes of emitted nitrogen atoms are larger than the time for thermoluminescence registration (~ 227–255 s) the thermoluminescence maxima were shifted to the higher temperatures compared to the position of the maximum of vortex density in He II for the conditions of our experiments [38].

3.3. Electron spin resonance investigations of nitrogen atoms stabilized in nitrogen–neon and nitrogen–argon nanoclusters

We performed investigations of nitrogen atoms stabilized in ensembles of nitrogen–neon and nitrogen–argon nanoclusters immersed in He II by the ESR method. The ESR spectra of nitrogen atoms were obtained for all samples studied in this work. The ESR spectra were initially recorded for as-prepared samples at $T \sim 1.32$ K and later again after warming up to temperature 2.16 K and cooling back to $T \sim 1.32$ K. During the warming processes, registration of thermoluminescence of the samples were recorded. Figure 8 shows examples of ESR spectra of nitrogen

Adil Meraki, Patrick T. McColgan, Sergei Sheludiakov, David M. Lee, and Vladimir V. Khmelenko
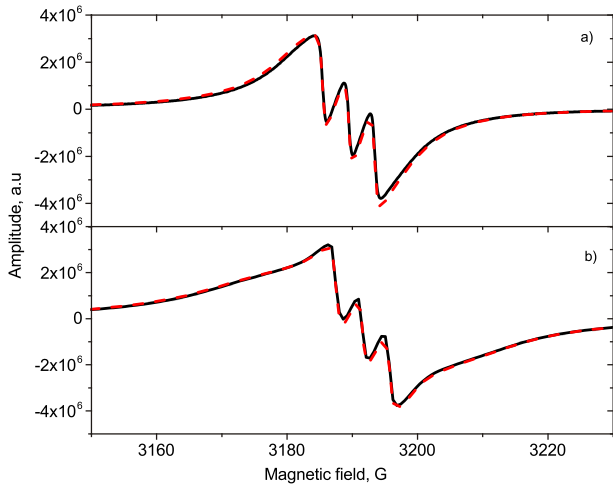
Fig. 8. (Color online) Comparison of the ESR spectra for as-prepared ensembles of nanoclusters taken at $T = 1.32$ K (black solid line) and after completing cycle of warming to 2.16 K and cooling back to $T = 1.32$ K (red dashed line). Spectra were obtained for samples prepared from nitrogen–neon–helium mixture $[N_2]/[Ne]/[He] = 1/1/100$ (a), and nitrogen–argon–helium mixture $[N_2]/[Ar]/[He] = 1/1/200$ (b).

Fig. 9. Dependence of the average concentration of N atoms stabilized in nitrogen–neon and nitrogen–argon nanoclusters on the N_2/Ne (blue line with triangles) and N_2/Ar (blue line with circles) ratios in gas mixtures. Dependence of the integrated α-group intensity of nitrogen atoms during the warming in ensembles of nitrogen–neon and nitrogen–argon nanoclusters on the N_2/Ne (red line with triangles) and N_2/Ar (red line with circles) ratios in gas mixtures. Arrows correspond to right and left hand vertical scales, respectively.

atoms stabilized in nitrogen–neon and nitrogen–argon nanoclusters. As can be seen from this figure the annealing of the samples immersed in He II to temperature 2.16 K does not change the ESR spectra. It means that there is no change in the concentrations of N atoms in the samples according to our ESR measurements. Although concentrations of stabilized nitrogen atoms do not show any change during process of warming up nitrogen–neon and nitrogen–argon nanoclusters as indicated from ESR measurements (see Fig. 8), it is known that total number of emitted photons during the entire process of warming up is five orders magnitude less than the number of stabilized atoms [38]. Thus ESR measurements cannot detect such small changes of nitrogen atom concentrations during the warming and cooling. From analysis of ESR spectra we determined average and local concentrations of nitrogen atoms in the samples [40]. The
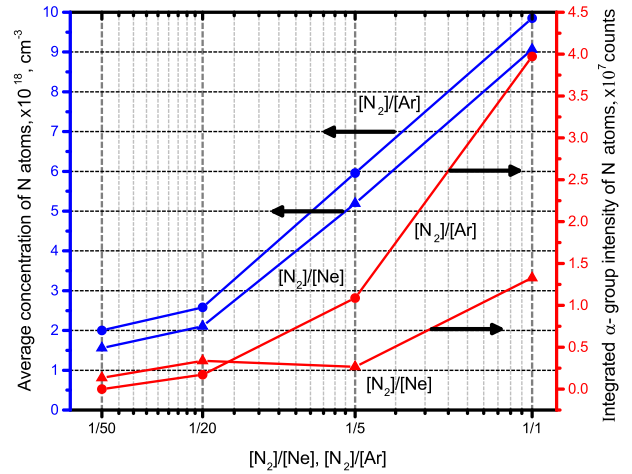
estimated values of average and local concentrations of nitrogen atoms in ensembles of nitrogen–neon and nitrogen–argon nanoclusters are shown in Table 1 and Table 2, respectively.

Figure 9 shows dependence of the average concentration of N atoms and dependence of the integrated α-group intensity of N atoms stabilized in ensembles of nitrogen–neon and nitrogen–argon nanoclusters on the N_2/Ne and N_2/Ar ratios in gas mixtures used for their preparation. One can see from Fig. 9 that there is a correlation between dependence of the average concentration of nitrogen atoms stabilized in the as-prepared ensembles of nitrogen–neon and nitrogen–argon nanoclusters and dependence of the N atom α-group emission intensity integrated over the entire warming period for these ensembles.

Table 1. Average and local concentrations of nitrogen atoms stabilized in the ensembles of nitrogen–neon nanoclusters

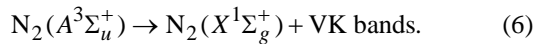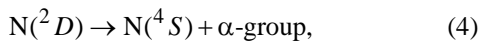| Gas mixture used for formation of nitrogen–neon nanoclusters, $[N_2]/[Ne]/[He]$	1/1/50	1/5/100	1/20/400	1/50/1000
Average concentration, cm^{-3}	$9.06 \cdot 10^{18}$	$5.19 \cdot 10^{18}$	$2.11 \cdot 10^{18}$	$1.56 \cdot 10^{18}$
Local concentration, cm^{-3}	$3.42 \cdot 10^{20}$	$2.87 \cdot 10^{20}$	$3.19 \cdot 10^{20}$	$2.66 \cdot 10^{20}$

Table 2. Average and local concentrations of nitrogen atoms in the ensembles of nitrogen–argon nanoclusters

Gas mixture used for formation of nitrogen–argon nanoclusters, $[N_2]/[Ar]/[He]$	1/1/200	1/5/600	1/20/2000	1/50/5000
Average concentration, cm^{-3}	$9.85 \cdot 10^{18}$	$5.96 \cdot 10^{18}$	$2.58 \cdot 10^{18}$	$2.00 \cdot 10^{18}$
Local concentration, cm^{-3}	$3.12 \cdot 10^{20}$	$3.29 \cdot 10^{20}$	$1.75 \cdot 10^{20}$	$1.69 \cdot 10^{20}$

4. Discussion

Ensembles of nanoclusters immersed in He II represent a new class of non-crystalline nanomaterials formed by injecting a beam composed of helium and impurity gases into superfluid helium ^{4}He. When the gas jet meets the surface of the superfluid helium, the formation of nanoclusters, each surrounded by one or two layers of solid helium due to Van der Waal forces, occurs inside superfluid helium. Matrix isolation of highly reactive atoms in nanoclusters leads to high concentrations of these atoms. Upon the injection of impurity particles into bulk superfluid helium, a shell structures of nanoclusters are formed in such a way that heavier impurities form cores of nanoclusters which are surrounded by shells of lighter impurities [19,40,41].

The dynamics of thermoluminescence spectra collected during the warming of ensembles of nanoclusters immersed into He II differ from the spectra that accompanied their destruction after removal from liquid helium discussed previously [23]. Increasing the temperature of the sample led to intense luminescence. At the beginning of the warm up, we observed emissions from the α-group of N atoms, the VK bands of N_2 molecules, and also the β-groups of O atoms. We suggest that recombination of nitrogen atoms in the ground ^4S state is the main source of the excitation of atoms and molecules during the sample warming since the excitations from metastable $N_2(A^3\Sigma_u^+)$ were efficiently transferred to the $N(^4S)$ and $O(^3P)$ atoms, resulting in the formation of the ^2D state of N atoms and the ^1S state of O atoms. Some of the metastable $N_2(A^3\Sigma_u^+)$ molecules emitted light, producing VK bands. All processes leading to light emission can be described by the following equations:

$$N(^4S) + N(^4S) \rightarrow N_2(A^3\Sigma_u^+), \qquad (1)$$

$$N_2(A^3\Sigma_u^+) + N(^4S) \rightarrow N(^2D) + N_2(X^1\Sigma_g^+), \qquad (2)$$

$$N_2(A^3\Sigma_u^+) + O(^3P) \rightarrow O(^1S) + N_2(X^1\Sigma_g^+), \qquad (3)$$

$$N(^2D) \rightarrow N(^4S) + \alpha\text{-group}, \qquad (4)$$

$$O(^1S) \rightarrow O(^1D) + \beta\text{-group}, \qquad (5)$$

$$N_2(A^3\Sigma_u^+) \rightarrow N_2(X^1\Sigma_g^+) + \text{VK bands}. \qquad (6)$$
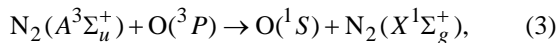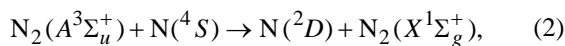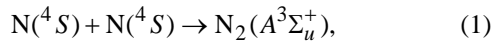
The glowing of the ensembles of nanoclusters immersed in He II increased in intensity with increasing temperature, and reached maxima at ~ 1.9 K. It should be pointed out that for most of the observed thermoluminescence curves the position of the maxima does not depend on concentration of nitrogen atoms stabilized in the sample prepared from different gas mixtures (see Figs. 3 and 7). The average concentrations of nitrogen atoms in these samples are in the range from $\sim 10^{18}$ to 10^{19} (see Tables 1 and 2).

During the sample warming the overall integrated emission of intensity of the α-group increases with increasing concentration of nitrogen atoms in the samples (see Fig. 9). On the other hand, the characteristics of the dynamics of the thermoluminescence spectra are almost the same for ensembles of nanoclusters with different concentrations of stabilized nitrogen atoms. Thus, it can be concluded that processes of explosive releases of the stored energy in the nanoclusters are not responsible for the observed dynamics of the thermoluminescence.

Now we shall discuss the features of the emission spectra of nitrogen–neon nanoclusters immersed into He II. In previous work the effect of oxygen impurities on the luminescence spectra of nitrogen nanoclusters during their destruction was investigated [23]. In the present work, we also observed the influence of oxygen impurities on the luminescence spectra of nitrogen–neon nanoclusters immersed into superfluid helium during the warm up. The M-bands of NO molecules were absent in the integrated spectra for the nanoclusters prepared from gas mixture $N_2/Ne/He = 1/1/100$ ($O_2/N_2 = 10^{-4}$ due to contamination of oxygen in the helium gas) as presented in Fig. 6(a). However, increasing the ratio of O_2/N_2 from 10^{-4} to $4 \cdot 10^{-4}$ in the ensembles of nanoclusters prepared from gas mixture $N_2/Ne/He = 1/20/400$ led to the appearance of the M-bands of NO molecules. Similar results are also seen for the case of nitrogen–argon nanoclusters prepared from the gas mixtures $N_2/Ar/He = 1/1/200$, and $N_2/Ar/He = 1/5/600$ (see Fig. 4). We suggest that the NO molecules were formed as a result of recombination of $N(^4S)$ and $O(^3P)$ atoms, leading to the appearance of NO emission, according to the following processes:

$$N(^4S) + O(^3P) \rightarrow NO(a^4\Pi), \qquad (7)$$

$$NO(a^4\Pi) \rightarrow NO(X^2\Pi) + h\nu \ (M\text{-bands}). \qquad (8)$$
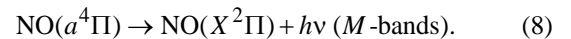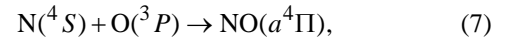
In addition to the appearance of the M-bands of NO, the emission of the First Positive system of N_2 molecules was also detected for this sample as seen in Fig. 6(b). The presence of the excited $N_2(B^3\Pi_g)$ state might be explained by the fact that the B state has vibrationally resonant levels with $N_2(A^3\Sigma_u^+)$ state.

For the case of the nitrogen–neon nanoclusters prepared from the gas mixture $N_2/Ne/He = 1/1/100$ the positions of VK bands of N_2 molecules shows that the emission occurs from the N_2 matrix. On the other hand, for the case of nanoclusters prepared from the gas mixtures $N_2/Ne/He = 1/20/400$ and $N_2/Ne/He = 1/50/1000$ the VK bands of N_2 and the M-band of NO positions correspond to those obtained for Ne matrices. The position of the α-group also reveals influence of the environment on the emission spectra of N atoms during warming of nanoclusters. The α-group spectra in the integrated spectra during the warm-up for the nanoclusters prepared from the gas mixture $N_2/Ne/He = 1/1/100$ had a maximum at 522 nm, whereas for the case

of the nanoclusters prepared from the gas mixture N_2/Ne/He = 1/20/400, and N_2/Ne/He = 1/50/1000 the peaks were detected at 521 and 520 nm, respectively. This feature of the spectrum leads to the conclusion that during the warming of the sample prepared from the N_2/Ne/He = = 1/1/100 gas mixture the emitting $N(^2D)$ atoms were surrounded mostly by N_2 molecules, while during the warming of nanoclusters prepared from the gas mixture N_2/Ne/He = = 1/20/400 and N_2/Ne/He = 1/50/1000 the N atoms and NO molecules were surrounded mostly by Ne atoms. This interpretation is in reasonable agreement with the differences in the dynamics of the α-group emission observed in Fig. 7. The differences of the temperature dependence of the α-group emission apparently result from the differences in the environments of the $N(^2D)$ metastable atom in the nanoclusters. Typical decay times of the α-group for Ne-containing nanoclusters are noticeably longer than for N_2 matrices. For the samples obtained by condensation of N_2/Ne/He mixtures, the decay time of the α-group is ~300 s, whereas for the N_2 matrices it is only ~30 s [24].

All of the above mentioned chemical processes proceed inside superfluid helium. The nitrogen molecules are formed as a result of recombination of pairs of nitrogen atoms with the energy close to dissociation limit in high vibrational levels. The vibration relaxation of N_2 molecules in solid N_2 is rather slow (a few seconds) [42–44]. During this long relaxation time all energy released as phonons can be easy removed by superfluid helium surrounding nanoclusters [45]. The main question here is how to explain chemical reactions of heavy atoms (nitrogen and oxygen) at temperatures in the range 1.1–2.16 K when diffusion of these atoms in a solid N_2 matrix is completely suppressed.

Thermoluminescence of solid nitrogen containing stabilized nitrogen atoms was explained by processes of diffusion and recombination of stabilized atoms. At the temperatures of our experiments ($T \sim$ 1.2–2.16 K), diffusion of nitrogen atoms in solid N_2 and solidified rare gases are completely suppressed. The phenomenon observed earlier of thermoluminescence of nanoclusters containing stabilized atoms immersed in He II was explained by different mechanisms. The first mechanism suggested that during injection of atoms and molecules from gas phase into bulk superfluid helium, single $N(^2D)$ metastable atoms and N_2 molecules can be captured in solidified helium shells [24]. In the helium shells the lifetime of $N(^2D)$ atom is close to that of free $N(^2D)$ atom (~ 24 h). Thus in this model, N atoms and molecules are each surrounded by solid helium. Raising temperature activates atomic and molecular diffusion through solidified helium which leads to formation of $N(^2D)$–N_2 Van der Waals complexes. In these complexes the lifetime of $N(^2D)$ atoms became much shorter (~ 30 s) resulting in observation of luminescence of the α-group [24]. On the other hand, x-ray and ultrasound studies of samples formed in superfluid helium provide strong evidence that the samples consist of collections of nano-

clusters which form porous structures inside superfluid helium [14–17]. The observation of only nanoclusters in the samples rules out the presence of nitrogen atoms and molecules isolated in solid helium, so the first model does not provide an explanation of the observed phenomenon.

The second mechanism suggested was that electrons and nitrogen ions can be captured separately in molecular nitrogen nanoclusters during the processes of injection of discharge products in He II at T = 1.5 K [25]. Increasing the temperature of the ensembles of nanoclusters immersed into He II could initiate release of electrons from the traps. Following that, the electrons tunnel through the nanoclusters resulting in electron–ion neutralization reactions. The energy from excited molecules can be emitted as light or travel through the N_2 matrix to stabilized nitrogen atoms leading to formation $N(^2D)$ atoms with the resulting emission of the α-group.

However, in our experiments we did not observed any ESR signal from electrons in the samples stored in He II. Moreover none of the above described mechanisms could explain the temperature dependence of the thermoluminescence observed in this and our previous work [38]. Only the model suggested in Ref. 38 provides a reasonable explanation of the chemical reactions of heavy atoms in He II and the temperature dependence of thermoluminescence for ensembles of nitrogen nanoclusters immersed in He II. According to this model recombination of atoms residing on surfaces of nanoclusters occurs in the vortex cores of He II. Free nanoclusters and strands of nanoclusters are entrained into the vortex cores, where the collisions of nanoclusters increased substantially compared to that outside of vortex cores. Collisions of nanoclusters in the vortex cores can result in recombination of nitrogen and oxygen atoms residing on the surfaces of nanoclusters so entrained. Recombination of atoms leads to formation of excited nitrogen molecules which can emit light (VK bands) or transfer energy through chains of N_2 molecules to stabilized nitrogen atoms with subsequent emission of these atoms. Intensity of the thermoluminescence should be proportional to the density of vortices in He II. Figure 9 shows a correlation between the integrated intensities of α-group emission of N atoms and concentrations of stabilized nitrogen atoms in these samples. This correlation provides support for the connection between thermoluminescence of nanoclusters and chemical reactions of nitrogen atoms entrained into vortex cores.

Other experimental observations which support this model are shown in Fig. 10. Figure 10 presents the temperature dependences of the intensity of thermoluminescence of nitrogen–neon, nitrogen–argon and nitrogen nanoclusters immersed in He II. In this figure the temperature dependence of the vortex density in bulk helium is also shown. The vortex density, L, in bulk He II was estimated from equation

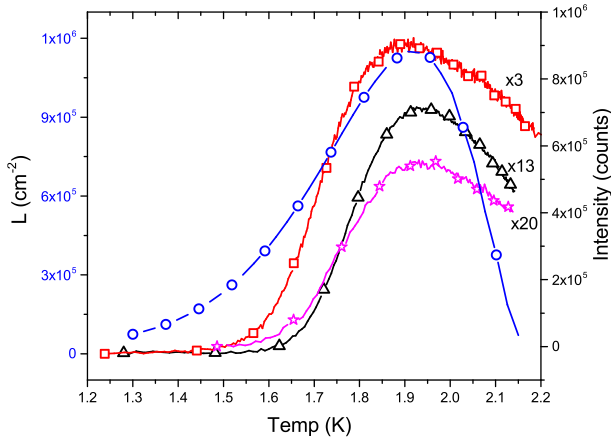$$L^{1/2} = \gamma(T)u_{ns}, \tag{9}$$

Fig. 10. (Color online) Dependence of vortex density in superfluid helium, *L*, on temperature during observation of thermoluminescence from the ensemble of nitrogen nanoclusters (circles) [38] and temperature dependences of thermoluminescence intensity of α-group nitrogen atoms for the different samples formed from [N_2]/[He] = 1/400 (squares), [N_2]/[Ar]/[He] = 1/1/200 (triangles), [N_2]/[Ne]/[He] = 1/1/100 (stars) gas mixtures.

where u_{ns} is the relative velocity of the normal and superfluid components, and the coefficient $\gamma(T)$ has been measured experimentally [31]. For counterflow, u_{ns} is related to the applied heat flux q according to

$$u_{ns} = \frac{q}{\rho_s sT},$$ (10)

where ρ_s is the superfluid density and s is the specific entropy of He II. The resulting flux density is given by

$$L^{1/2} = \gamma(T) \frac{q}{\rho_s sT}.$$ (11)

In the case of applying a temperature gradient, dT/dx, the heat flux is described by the Gorter–Mellink heat transport formula

$$q = -\left[f^{-1}(T, P) \frac{dT}{dx} \right]^{1/3},$$ (12)

where

$$f^{-1}(T, P) = f^{-1}(T_\lambda, P) \left\{ \left(\frac{T}{T_\lambda} \right)^{5.7} \left[1 - \left(\frac{T}{T_\lambda} \right)^{5.7} \right] \right\}^3$$ (13)

is the heat conductivity function for turbulent flow [46]. If we also consider the dependence on temperature of the superfluid density of helium in the temperature range 1.1–2.16 K

$$\rho_s = \rho \left[1 - \left(\frac{T}{T_\lambda} \right)^{5.6} \right],$$ (14)

and specific entropy of superfluid helium

$$s = 1.5838 \left(\frac{T}{T_\lambda} \right)^{5.6}$$ (15)

we can obtain a graph of the dependence of the vortex density on temperature for the experimentally measured temperature gradient in superfluid helium for the conditions of our experiments as shown in Fig. 1(b) of Ref. 38. As can be seen from Fig. 10, the temperature dependences of the thermoluminescence intensity for all studied ensembles of nanoclusters are very similar to that of the vortex density in bulk He II. All dependences have maxima at $T \sim 1.9$ K. This similarity strongly supports our model of thermoluminescence of nanoclusters resulting from chemical reactions of nitrogen atoms initiated by attraction of nanoclusters in vortex cores in He II.

Recently we performed investigations of the influence of the rotation speed of a beaker containing superfluid helium on the intensity of luminescence of collections of nitrogen nanoclusters during their injection into He II [47]. We observed correlations between the rotation speed of the beaker with He II and the luminescence intensity of nitrogen atoms in molecular nitrogen nanoclusters. The increase of the luminescence intensity with increase of rotation speed was explained by the initiation of chemical reactions of nitrogen atoms on the surfaces of nanoclusters entrained inside vortex cores. These experiments also support the model of thermoluminescence initiated by quantum vortices in He II.

It is also known that thermoluminescence was observed only during warming up as-prepared ensembles of nanoclusters [38]. All following processes of warming up after cooling do not provide any additional thermoluminescence. This means that all free nanoclusters and free strands of nanoclusters are efficiently captured in the vortex cores in first warming and participated in chemical reactions resulting in chemical bondings of almost all free nanoclusters. Thus they cannot further participate in chemical reactions after the first warming.

In summary, in this work we carried out a study of nitrogen atoms stabilized in nanoclusters of molecular nitrogen with different admixtures of Ar and Ne. Similar to our previous work, we observed maxima of thermoluminescence of nitrogen atoms at $T = 1.9$ K which did not depend on the sample composition. This observation provides evidence for initiation of thermoluminescence by quantum vortices in He II.

5. Conclusions

1. Ensembles of nitrogen–neon and nitrogen–argon nanoclusters immersed in He II were studied by optical and ESR spectroscopies during warming up from 1.32 to 2.16 K. It was found that the temperature dependence of thermoluminescence of these ensembles shows a maximum intensity at $T \sim 1.9$ K similar to temperature dependence of the vortex density in He II in this temperature range.

2. Results obtained in this work provide additional evidence for a mechanism of thermoluminescence involving chemical reactions of nitrogen atoms residing on surfaces of nanoclusters. These reactions occur in the vortex cores of He II which efficiently entrained nanoclusters and free strands of nanoclusters.

3. These studies open new possibilities for investigation of chemical reactions of heavy atoms and free radicals initiated by vortices in He II, under the conditions where diffusion and tunneling of reagents in solid noncrystalline samples are completely suppressed.

4. The approach used in this work provides new possibilities for synthesis of exotic species in nanoclusters at low temperatures.

Acknowledgments

———————

1. R.A. Ruehrwein, J.S. Hashma, and J.W. Edwards, *J. Phys. Chem.* **64**, 1317 (1960).

2. B.J. Fontana, *J. Appl. Phys.* **29**, 1668 (1958).

3. B.J. Fontana, *J. Chem. Phys.* **31**, 148 (1959).

4. B. Brocklehurst and G.C. Pimentel, *J. Chem. Phys.* **36**, 2040 (1962).

5. B. Tribollet and F. Valadier, *J. Phys. France* **42**, 673 (1981).

6. D.S. Tinti and G.W. Robinson, *J. Chem. Phys.* **49**, 3229 (1968).

7. R.J. Sayer, R.H. Prince, and W.W. Duley, *Phys. Status Solidi B* **106**, 249 (1981).

8. E. Savchenko, I. Khyzhniy, S. Uyutnov, A. Barabashov, G. Gumenchuk, M.K. Beyer, A. Ponomaryov, and V. Bondybey, *J. Phys. Chem. A* **119**, 2475 (2015).

9. A.N. Ponomarev, E.V. Savchenko, I.V. Khizhniy, G.B. Gumenchuk, M. Frankowski, and V.E. Bondybey, *Fiz. Nizk. Temp.* **33**, 705 (2007) [*Low Temp. Phys.* **33**, 532 (2007)].

10. E.B. Gordon, V.V. Khmelenko, E.A. Popov, A.A. Pelmenev, and O.F. Pugachev, *Chem. Phys. Lett.* **155**, 301 (1989).

11. E.B. Gordon, L.P. Mezhov-Deglin, and O.F. Pugachev, *JETP Lett.* **19**, 63 (1974).

12. E.B. Gordon, L.P. Mezhov-Deglin, O.F. Pugachev, and V.V. Khmelenko, *Cryogenics* **16**, 555 (1976).

13. V. Kiryukhin, B. Keimer, R.E. Boltnev, V.V. Khmelenko, and E.B. Gordon, *Phys. Rev. Lett.* **79**, 1774 (1997).

14. S.I. Kiselev, V.V. Khmelenko, D.M. Lee, V. Kiryukhin, R.E. Boltnev, E.B. Gordon, and B. Keimer, *Phys. Rev. B* **65**, 024517 (2002).

15. E.P. Bernard, R.E. Boltnev, V.V. Khmelenko, V. Kiryukhin, S.I. Kieselev, and D.M. Lee, *Phys. Rev. B* **69**, 104201 (2004).

16. V. Kiryukhin, E.B. Bernard, V.V. Khmelenko, R.E. Boltnev, N.V. Krainyukova, and D.M. Lee, *Phys. Rev. Lett.* **98**, 195506 (2007).

17. N.V. Krainyukova, R.E. Boltnev, E.P. Bernard, V.V. Khmelenko, V. Kiryukhin, and D.M. Lee, *Phys. Rev. Lett.* **109**, 245505 (2012).

18. E.P. Bernard, V.V. Khmelenko, and D.M. Lee, *J. Low Temp. Phys.* **150**, 516 (2008).

19. S. Mao, R.E. Boltnev, V.V. Khmelenko, and D.M. Lee, *Fiz. Nizk. Temp.* **38**, 1513 (2012) [*Low Temp. Phys.* **38**, 1037 (2012)].

20. E.B. Gordon, L.P. Mezhov-Deglin, O.F. Pugachev, and V.V. Khmelenko, *Sov. Phys. JETP* **46**, 502 (1977).

21. R.E. Boltnev, E.B. Gordon, I.N. Krushinskaya, M.V. Marynenko, A.A. Pelmenev, E.A. Popov, V.V. Khmelenko, and A.F. Shestakov, *Fiz. Nizk. Temp.* **23**, 753 (1997) [*Low Temp. Phys.* **23**, 567 (1997)].

22. V.V. Khmelenko, D.M. Lee, I.N. Krushinskaya, R.E. Boltnev, I.B. Bykhalo, and A.A. Pelmenev, *Fiz. Nizk. Temp.* **38**, 871 (2012) [*Low Temp. Phys.* **38**, 688 (2012)].

23. A. Meraki, S. Mao, P.T. McColgan, R.E. Boltnev, D.M. Lee, and V.V. Khmelenko, *J. Low Temp. Phys.* **158**, 468 (2016).

24. R.E. Boltnev, E.B. Gordon, V.V. Khmelenko, I.N. Krushinskaya, M.V. Marynenko, A.A. Pelmenev, E.A. Popov, and A.F. Shestakov, *Chem. Phys.* **189**, 367 (1994).

25. A.A. Pelmenev, I.N. Krushinskaya, I.B. Bykhalo, and R.E. Boltnev, *Fiz. Nizk. Temp.* **42**, 289 (2016) [*Low Temp. Phys.* **42**, 224 (2016)].

26. W.F. Vinen, *J. Low Temp. Phys.* **145**, 7 (2006).

27. C.F. Barenghi, L. Skrbek, and K.R. Sreenivasan, *PNAS* **111**, 4647 (2014).

28. Y.A. Sergeev and C.F. Barenghi, *J. Low Temp. Phys.* **157**, 429 (2009).

29. 10 G.P. Bewley, D.P. Lathrop, and K.R. Sreenivasan, *Nature* **441**, 588 (2006).

30. W. Guo, J.D. Wright, S.B. Cahn, J.A. Nikkel, and D.N. McKinsey, *Phys. Rev. Lett.* **102**, 235301 (2009).

31. S. Babuin, M. Stammeier, E. Varga, M. Rotter, and L. Skrbek, *Phys. Rev. B* **86**, 134515 (2012).

32. D.E. Zmeev, F. Pakpour, P.M. Walmsley, A.I. Golov, W. Guo, D.N. McKinsey, G.G. Ihas, P.V.E. McClintock, S.N. Fisher, and W.F. Vinen, *Phys. Rev. Lett.* **110**, 175303 (2013).

33. W. Guo, M. LaMantia, D.P. Lathrop, and S.W.V. Sciver, *PNAS* **111**, 4653 (2014).

34. G.P. Bewley, M.S. Paoletti, K.R. Sreenivasan, and D.P. Lathrop, *PNAS* **105**, 13707 (2008).

35. E. Fonda, D.P. Meichle, N.T. Ouellette, S. Hormoz, and D.P. Lathrop, *PNAS* **111**, 4707 (2014).

36. E.B. Gordon, A.V. Karabulin, V.I. . Matyushenko, V.D. Sizov, and I.I. Khodos, *J. Exp. Theor. Phys.* **112**, 1061 (2011).

37. E.B. Gordon, A.V. Karabulin, V.I. Matyushenko, V.D. Sizov, and I.I. Khodos, *Chem. Phys. Lett.* **519**–**520**, 64 (2014).

38. A. Meraki, P.T. McColgan, P.M. Rentzepis, R.Z. Li, D.M. Lee, and V.V. Khmelenko, *Phys. Rev. B* **95**, 1045026 (2017).

39. S. Mao, A. Meraki, P.T. McColgan, V. Shemelin, V.V. Khmelenko, and D.M. Lee, *Rev. Sci. Instrum.* **85**, 073906 (2014).

40. A. Meraki, P.T. McColgan, R.E. Boltnev, D.M. Lee, and V.V. Khmelenko, *J. Low Temp. Phys.* **192**, 228 (2018).

41. E.B. Gordon, *Fiz. Nizk. Temp.* **30**, 1009 (2004) [*Low Temp. Phys.* **30**, 756 (2004)].

42. A.A. Ovchinnikov, *Sov. Phys. JETP* **30**, 147 (1970).

43. K. Dressler, O. Oehler, and D.A. Smith, *Phys. Rev. Lett.* **34**, 1364 (1975).

44. K. Takizawa, A. Takami, and S. Koda, *J. Phys. Chem. A* **104**, 3693 (2000).

45. V. Arp, *Cryogenics* **10**, 96 (1970).

46. S.W.V. Sciver, *Trans ASME: J. Heat Transfer.* **121**, 142 (1999).

47. P.T. McColgan, S. Sheludiakov, D.M. Lee, and V.V. Khmelenko, *Fiz. Nizk. Temp.* **45**, 356 (2019) [*Low Temp. Phys.* **45**, 310 (2019)].

———————————————————

Термолюмінесценція азотно-неонових і азотно-аргонових нанокластерів, занурених у надплинний гелій

A. Meraki, P.T. McColgan,
С. Шелудяков, D.M. Lee,
В.В. Хмеленко

Ансамблі нанокластерів, отримані введенням в надплинний гелій молекул і атомів азоту, а також атомів інертних газів (Ne і Ar), вивчено методами спектроскопії електронного спінового резонансу та оптичної спектроскопії. Досліджено динаміку спектра термолюмінесценції під час розігріву пористих структур, сформованих азот-неоновими та азот-аргоновими нанокластерами всередині надплинного гелію. Наведено експериментальні докази того, що квантові вихори ініціюють хімічні реакції в пористих ансамблях нанокластерів. Використання даного експериментального підходу дозволяє вивчати хімічні реакції важких атомів і молекул при таких низьких температурах, коли їх дифузія і квантове тунелювання повністю пригнічені.

Ключові слова: термолюмінесценція, пористі структури, нанокластери, надплинний гелій.

Термолюминесценция азотно-неоновых и азотно-аргоновых нанокластеров, погруженных в сверхтекучий гелий

A. Meraki, P.T. McColgan,
С. Шелудяков, D.M. Lee,
В.В. Хмеленко

Ансамбли нанокластеров, полученные введением в сверхтекучий гелий молекул и атомов азота, а также атомов инертных газов (Ne и Ar), изучены методами спектроскопии электронного спинового резонанса и оптической спектроскопии. Исследована динамика спектра термолюминесценции во время разогрева пористых структур, сформированных азот-неоновыми и азот-аргоновыми нанокластерами внутри сверхтекучего гелия. Приведены экспериментальные доказательства того, что квантовые вихри инициируют химические реакции в пористых ансамблях нанокластеров. Использование данного экспериментального подхода позволяет изучать химические реакции тяжелых атомов и молекул при таких низких температурах, когда их диффузия и квантовое туннелирование полностью подавлены.

Ключевые слова: термолюминесценция, пористые структуры, нанокластеры, сверхтекучий гелий.